Journal of Orthopaedic Translation 44 (2024) 139–154

Contents lists available at ScienceDirect

Journal of Orthopaedic Translation

journal homepage: www.journals.elsevier.com/journal-of-orthopaedic-translation

Inhibition of PI3K/AKT signaling pathway prevents blood-induced heterotopic ossification of the injured tendon

Xuri Chen [a,b,c,d,1], Yuwei Yang [a,b,c,d,1], Yuqing Gu [a,b,c,d], Junzhi Yi [a,b,c,d], Wenyu Yao [a], Zhuomin Sha [a], Hongwei Wu [a,b,c,d], Yunting Zhou [a], Zhonglin Wu [a,b,c,d], Fangyuan Bao [a,b,c,d], Jiasheng Wang [a,b,c,d], Ying Wang [a,b,c,d], Yuanhao Xie [a,b,c,d], Chenlu Gao [a], Boon Chin Heng [f], Hua Liu [a,b,c,d,e], Zi Yin [b,c,d,e], Xiao Chen [a,b,c,d,e], Jing Zhou [a,b,c,d,e,**], Hongwei Ouyang [a,,c,d,e,*]

[a] *Dr. Li Dak Sum & Yip Yio Chin Center for Stem Cells and Regenerative Medicine, and Department of Orthopedic Surgery of the Second Affiliated Hospital, Zhejiang University School of Medicine, Hangzhou, 310058, China*
[b] *Liangzhu Laboratory, Zhejiang University, 1369 West Wenyi Road, Hangzhou, 311121, China*
[c] *Department of Sports Medicine, Zhejiang University School of Medicine, Hangzhou, 310058, China*
[d] *Zhejiang University-University of Edinburgh Institute, Zhejiang University School of Medicine, and Key Laboratory of Tissue Engineering and Regenerative Medicine of Zhejiang Province, Zhejiang University School of Medicine, Hangzhou, 314400, China*
[e] *China Orthopedic Regenerative Medicine Group (CORMed), Hangzhou, 310058, China*
[f] *Central Laboratory, Peking University School and Hospital of Stomatology, Beijing, 100081, China*

ARTICLE INFO

Keywords:
Blood
Heterotopic ossification
Inflammation
PI3K/AKT signaling pathway
Tendon stem/progenitor cells

ABSTRACT

Objective: It is a common clinical phenomenon that blood infiltrates into the injured tendon caused by sports injuries, accidental injuries, and surgery. However, the role of blood infiltration into the injured tendon has not been investigated.

Methods: A blood-induced rat model was established and the impact of blood infiltration on inflammation and HO of the injured tendon was assessed. Cell adhesion, viability, apoptosis, and gene expression were measured to evaluate the effect of blood treatment on tendon stem/progenitor cells (TSPCs). Then RNA-seq was used to assess transcriptomic changes in tendons in a blood infiltration environment. At last, the small molecule drug PI3K inhibitor LY294002 was used for *in vivo* and *in vitro* HO treatment.

Results: Blood caused acute inflammation in the short term and more severe HO in the long term. Then we found that blood treatment increased cell apoptosis and decreased cell adhesion and tenonic gene expression of TSPCs. Furthermore, blood treatment promoted osteochondrogenic differentiation of TSPCs. Next, we used RNA-seq to find that the PI3K/AKT signaling pathway was activated in blood-treated tendon tissues. By inhibiting PI3K with a small molecule drug LY294002, the expression of osteochondrogenic genes was markedly downregulated while the expression of tenonic genes was significantly upregulated. At last, we also found that LY294002 treatment significantly reduced the tendon HO in the rat blood-induced model.

Conclusion: Our findings indicate that the upregulated PI3K/AKT signaling pathway is implicated in the aggravation of tendon HO. Therefore, inhibitors targeting the PI3K/AKT pathway would be a promising approach to treat blood-induced tendon HO.

The translational potential of this article: Inhibitors targeting the PI3K/AKT pathway would be a promising alternative treatment of

* Corresponding author. Dr. Li Dak Sum & Yip Yio Chin Center for Stem Cells and Regenerative Medicine, and Department of Orthopedic Surgery of the Second Affiliated Hospital, Zhejiang University School of Medicine, Hangzhou, 310058, China.
** Corresponding author. Dr. Li Dak Sum & Yip Yio Chin Center for Stem Cells and Regenerative Medicine, and Department of Orthopedic Surgery of the Second Affiliated Hospital, Zhejiang University School of Medicine, Hangzhou, 310058, China.
E-mail addresses: zhoujing@zju.edu.cn (J. Zhou), hwoy@zju.edu.cn (H. Ouyang).
[1] These authors contributed equally to this work.

https://doi.org/10.1016/j.jot.2023.11.003
Received 10 August 2023; Received in revised form 3 November 2023; Accepted 6 November 2023

tendon HO in clinical usage.

1. Introduction

Blood infiltration into the injured tendon is a common clinical phenomenon due to sports injuries, accidental injuries, and surgery. However, due to the unclear effects of blood on injured tendons, there is no other auxiliary treatment for bleeding caused by trauma except hemostasis at present.

During the process of bleeding, a large number of blood cells gather within the injured area, and the blood circulation brings together all kinds of cytokines, chemokines, and growth factors, which provoke a local immune response. Additionally, during clinical treatment of the musculoskeletal system, growth factors such as transforming growth factor-β1 (TGF-β1), platelet-derived growth factor (PDGF), and vascular endothelial growth factor (VEGF) in the blood may potentially trigger the synthesis of extracellular matrix and promote re-vascularization, thereby accelerating the tissue repair [1–3]. However, autologous blood injections have no additional benefit in the clinical treatment of tendinopathy [4,5]. Even worse, bleeding in hemophilic arthritis (HA) leads to a decrease in tensile properties of tendon [6], which thus indicates the potential negative effects of blood infiltration on the tendon. Collectively, the conflicting results in these studies underscore the complicated effects of blood infiltration environment on injured tendons.

Tendon tissue consists of a large number of extracellular matrix and a small number of cells [7]. Among them, the role of tendon stem/progenitor cells (TSPCs) in tendon development and healing has attracted wide interest among researchers. Bi et al. first identified TSPCs and proved that the molecular environment provided by the niche was essential for the proper maintenance and differentiation of TSPCs during tendon development and repair [8]. In addition, TSPCs exhibited a strong tendency to abnormal differentiation in the inflammatory niche [9]. However, no study to date has examined the role of blood on TSPCs, which would be a critical problem in basic and clinical research.

Heterotopic ossification (HO) is a dynamic pathologic process that includes trauma/injury, inflammation, mesenchymal stem cells (MSCs) recruitment, chondrogenic differentiation, and ossification formation [10]. Mechanical stimulus and injury are essential factors in HO pathologies, which are reported able to induce chondrogenic/osteogenic differentiation [11,12]. However, it remains unclear whether hemorrhage contributes to HO. Besides, cellular components play a significant role in tendon HO. Macrophages are key mediators that link inflammation and HO pathogenesis, which can promote MSCs osteochondrogenic differentiation and significantly contribute to the hypoxic microenvironment [13–15]. So far, various types of progenitors have been detected as the origin of HO, including TSPCs, circulating MSCs, and peripheral neural progenitor cells [16–20]. Among these cells, TSPCs are currently the most investigated cell type of interest in tendon HO.

In this work, we intended to analyse the role of blood on the HO of the injured tendon *in vivo*, *in vitro,* and *ex vivo* levels. First, we established a rat model of the injured tendon with blood infiltration and observed that blood infiltration could lead to an acute inflammatory response and aggravate ectopic ossification. We also found that blood treatment impaired survival and led to abnormal differentiation of TSPCs. RNA-seq revealed that upregulated PI3K/AKT pathway was involved in blood-treated tendon tissue. Therefore, we employed PI3K/AKT inhibitor LY294002 to treat TSPCs and found that it could reverse the aberrant differentiation of TSPCs caused by blood. This research makes an important contribution to understanding the role of blood on injured tendons. Targeting the PI3K/AKT signaling pathway is a promising approach for treating tendon HO.

2. Results

2.1. Blood infiltration induced acute inflammation of the injured tendon in the short term

Autologous blood or PBS were injected into the rat Achilles tendon, and tendons were collected and analyzed 3 days after injection. Hyperplastic tissue and blood vessels were observed clearly around the Achilles tendons from the autologous blood injection group on 3 days (Fig. 1a). Further histological results showed different tendon structures between the two groups (Fig. 1b and c). There were many cells gathered at the injection sites, including some red blood cells, which proved that the blood remained at the site of tendon injury after 3 days. The collagen structure of the tendon was also disordered, and some collagen fibers were even observed to be destroyed, which was considered as a characteristic of tendinitis [21]. But after PBS injection, the cells and matrix in the tendon did not seem to change significantly. To further confirm the occurrence of inflammation, we carried out immunofluorescence staining of the macrophage surface marker CD68 (Fig. 1d and e). The results showed that the percentage of CD68 positive cells in the whole blood treatment group was significantly higher than that in the PBS control group. To determine the inflammation-related effects of blood, gene expression levels of IL-1β and IL-10 were examined (Fig. 1f and g). Blood increased the expression levels of pro-inflammatory genes IL-1β and IL-10 in the injured tendons than PBS control. Moreover, the expression level of extracellular matrix degradation-related gene matrix metalloproteinase 9 (MMP9) was higher in the blood treatment group than PBS control group (Fig. 1h). Collectively, these results confirmed that the injection of whole blood into the Achilles tendon would lead to the aggregation of macrophages, induce severe acute inflammation, and cause tendon matrix degeneration.

2.2. Blood infiltration aggravated HO of the injured tendon in the long term

Six weeks after autologous whole blood injection, we found that the hyperplastic tissue and neovascularization had disappeared (Fig. 2a). This indicated that the acute severe inflammatory reaction had subsided after 6 weeks. In appearance, there was no significant difference between the two groups. Therefore, it was necessary to further analyse the long-term effects of whole blood treatment of injured tendons.

Studies have shown a close relationship between tendon HO and tendon injury [22]. Therefore, we next analysed the HO of rat Achilles tendon by micro-CT, performed three-dimensional reconstruction of Achilles tendon, and analysed the ratio and degree of ossification in tendons of whole blood treatment versus PBS control group. At 6 weeks post-treatment, 75.00 % of rats developed detectable HO in the autologous blood injection group, while only 58.33 % were detected in the PBS control group (Fig. 2b and c). The volume of HO in the three-dimensional reconstructed images was statistically analysed. It was found that the volume of tendon HO in the whole blood treatment group was larger than that in the PBS group at 6 weeks post-treatment (Fig. 2d). This proved that even a single short duration of whole blood treatment would have a greater long-term impact on the injured tendon, accelerating the development of HO.

To further confirm the effects of whole blood on the injured tendon, histological staining of the tendons was performed. At 6 weeks post-treatment, HE and Masson staining results of the blood injection group showed that the aggregation of chondrocyte-like cells appeared at the ossification site (Fig. 2e and f). The results of SO staining showed that part of the matrix in the ossification area of the whole blood treatment group was stained with Safranin O, indicating the existence of cartilage extracellular matrix in this area. In the PBS control group, the staining of tendon matrix was homogeneous, and the collagen fibers were arranged in order (Fig. 2g). These results thus confirmed that whole blood treatment induced endochondral ossification of tendon tissues.

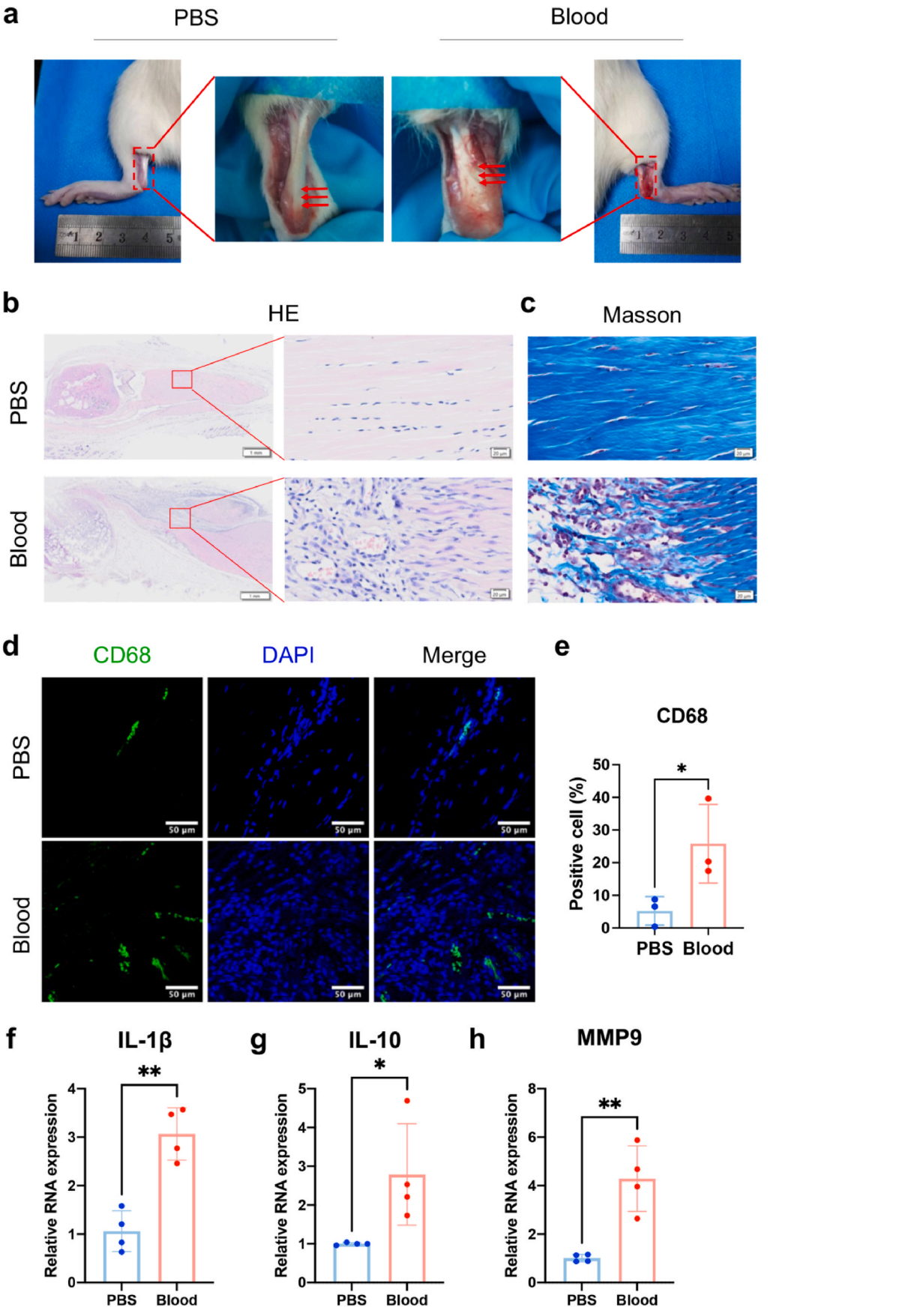

(caption on next page)

Fig. 1. Blood infiltration induced acute inflammation of the injured tendon in the short term. (a) Gross appearance of the Achilles tendon in the PBS and Blood groups on day 3. Red arrows indicate the specific injection site. (b, c) HE and Masson staining of the tendon in the PBS and Blood groups. Scale bar = 20 μm. (d, e) Immunofluorescence staining and quantitative analysis of CD68 (n = 3, unpaired t-test, *P < 0.05), Scale bar = 50 μm. (f–h) RT-qPCR of IL-1β, IL-10, and MMP9 expression (n = 4, unpaired t-test, *P < 0.05, **P < 0.01). (For interpretation of the references to colour in this figure legend, the reader is referred to the Web version of this article.)

To identify the characteristics of chondrocyte-like cells within the ossification area, we detected the protein expression of SOX9 and aggrecan (ACAN) in this area. The staining results showed that the expression of chondrogenic markers ACAN and SOX9 in the whole blood treatment group was significantly higher than that in the PBS control group (Fig. 2h, i, k, and l). Furthermore, the expression of tendon marker tenomodulin (TNMD) significantly decreased in the whole blood treatment group than PBS control group (Fig. 2j, m). These results suggested that after whole blood treatment, the expression of chondrogenic markers SOX9 and ACAN in the tendon was higher, which changed the cell phenotype in the tendon and accelerated the formation of tendon HO.

2.3. Blood treatment increased cell apoptosis and decreases cell adhesion and tenonic gene expression

Tendon tissue contains a small resident tendon stem cell population called TSPCs [23], which are also related to tendon ossification [24,25]. So, we isolated TSPCs from mouse tail tendons and identified them using colony formation unit assay, multi-differentiation assay, and flow cytometry analysis (Fig. S1) [8]. We performed a colony forming unit assay and found that TSPCs seeded at low density could generate viable colonies after 10 days, as visualized by crystal violet staining (Fig. S1a). After being cultured in an osteogenic/chondrogenic/adipogenic medium for 14 days, TSPCs were differentiated into osteocytes, chondrocytes, or adipocytes, revealed by deposit of calcium, glycosaminoglycan (GAG), or lipid droplets in the extracellular matrix, respectively (Fig. S1b). Also, TSPCs were positive for CD44, CD90.2, and Sca-1 and negative (≤10 %) for CD18, CD34, and CD45, which was consistent with the definition of TSPCs (Fig. S1c) [8].

To simulate the crosstalk between blood and TSPCs and to avoid the interference of blood cells, transwells were used for *in vitro* experiments. First, we tested the effect of different blood concentrations on TSPCs for 6 h (Figs. S2a and b). A slight increase in the number of adherent cells of TSPCs was observed under light microscopy in 10 % (v/v) and 20 % (v/v) of the blood compared to the control group. When the blood concentration increased to 40 % (v/v), the number of adherent cells began to decrease. In 80 % (v/v) blood, most of the cells were detached from the dish. So, we chose 20 % (v/v) blood as the treatment factor for further studies.

Then we treated TSPCs with 20 % (v/v) blood for 0, 6, 12, and 24 h using a transwell co-culture system to further explore the effects of whole blood treatment at different time on TSPCs. After removing the blood, cells were cultured for up to 72 h. With an increasing treatment time of blood, cell numbers were observed to be decreased. With 24 h of blood treatment, adherent cells were significantly reduced after 3 days of culture (Fig. 3a and b). This suggests that blood stimulation can reduce the adhesion capacity of TSPCs. Considering the decline in cell adhesion ability, we collected suspension cells by centrifugation after changing the culture medium for cell proliferation assay using the Cell Counting Kit-8 (CCK-8) assay. Surprisingly, 6 and 12 h of blood treatment enhanced cell proliferation (Fig. 3c). Longer time (24 h) blood treatment significantly reduced cell proliferation on day 3. These results demonstrated that 24 h of blood treatment inhibited the adhesion and proliferation of TSPCs, while 6 and 12 h blood treatment had the potential effect of promoting proliferation.

In general, cell proliferation and apoptosis are interrelated and balanced [26]. Based on the above results, we explored the effect of blood treatment on apoptosis and necrosis of TSPCs. Flow cytometry analysis showed that the number of early apoptotic cells (Annexin V single-positive) and late apoptotic/necrotic cells (Annexin V/PI double-positive staining) increased significantly with increasing blood treatment time (Fig. 3d–f). Thus, these results demonstrated that blood treatment could induce apoptosis and necrosis of TSPCs.

Next, we evaluated the effect of blood on TSPCs at the transcriptional level (Fig. 3g and h). After blood treatment, the expression of genes related to cell adhesion (Thbs4, Vcam1, and Itgb1) decreased significantly. This proved that blood treatment downregulated the expression of cell adhesion-related proteins, resulting in the decline of cell adhesion. The expression of anti-apoptotic gene Bcl2 [27] was also significantly downregulated, as well as tendon marker genes Scx, Mkx and Tnmd. Besides, the expression of Col1A1 decreased after 24 h blood treatment. However, 12 h of blood treatment increased the expression of Col1A1, which may be related to the short-term stress response of TSPCs to changes in the extracellular microenvironment [28]. To make a simple summary, blood treatment could induce apoptosis, decrease adhesion capacity, and downregulate the expression of tenonic genes of TSPCs in a time-dependent manner.

2.4. Blood treatment induced aberrant differentiation of TSPCs

To simulate the repair of injured tendons *in vivo*, we next studied the differentiation trend of TSPCs cultured in H-DMEM for 7 days (Fig. 4a). To determine the differentiation potential of TSPCs under blood treatment, the gene expression levels of each treatment group were compared (Fig. 4b). The RT-qPCR results showed that the gene expression of the chondrogenesis-related gene Sox9 was increased. Besides, the gene expression of osteogenesis-related genes such as osteocalcin (Ocn) and integrin-binding sialoprotein (Ibsp) was also increased in the blood treatment group. However, no apparent differences in osteogenesis-related gene Runx2 expression levels were detected among treatment groups. Furthermore, tenogenesis-related genes (Col1A1, Tnmd, Scx, and Mkx) decreased significantly with varying whole blood treatment time. Western blot results also showed that the SOX9 protein expression increased obviously after blood treatment and reached a relative peak at 12 h after blood treatment (Fig. 4c and d). Besides, we also detected alkaline phosphatase (ALP) activity of TSPCs under different blood treatment times when cultured in an osteogenic medium for 7 days. The results showed that ALP activity increased as early as 6 h of blood treatment (Fig. 4e and f). These results thus indicated that blood-treated TSPCs showed a tendency of chondrogenic and osteogenic differentiation, which was a cellular feature of ectopic endochondral ossification in tendon degenerative lesions [29,30].

2.5. Blood affected tendon tissues gene expression

To evaluate the impacts of blood on the tendon, transcriptome sequencing was also performed on the *ex vivo* tendon tissue. PCA projection showed that the global gene expression patterns between tendon tissues with and without blood treatment were distinguishable (Fig. 5a). 1078 DEGs, including 540 upregulated and 538 downregulated genes, were identified (Fig. 5b). Heatmap of differential gene cluster analysis revealed that gene expression changed between the two groups (Fig. 5c). These results demonstrated that tendon tissue had a certain response to blood treatment at the RNA level.

Kyoto Encyclopedia of Genes and Genomes (KEGG) pathway and Gene Ontology (GO) analyses were performed to determine the changes in cell metabolism and physiology after blood treatment. The pathways

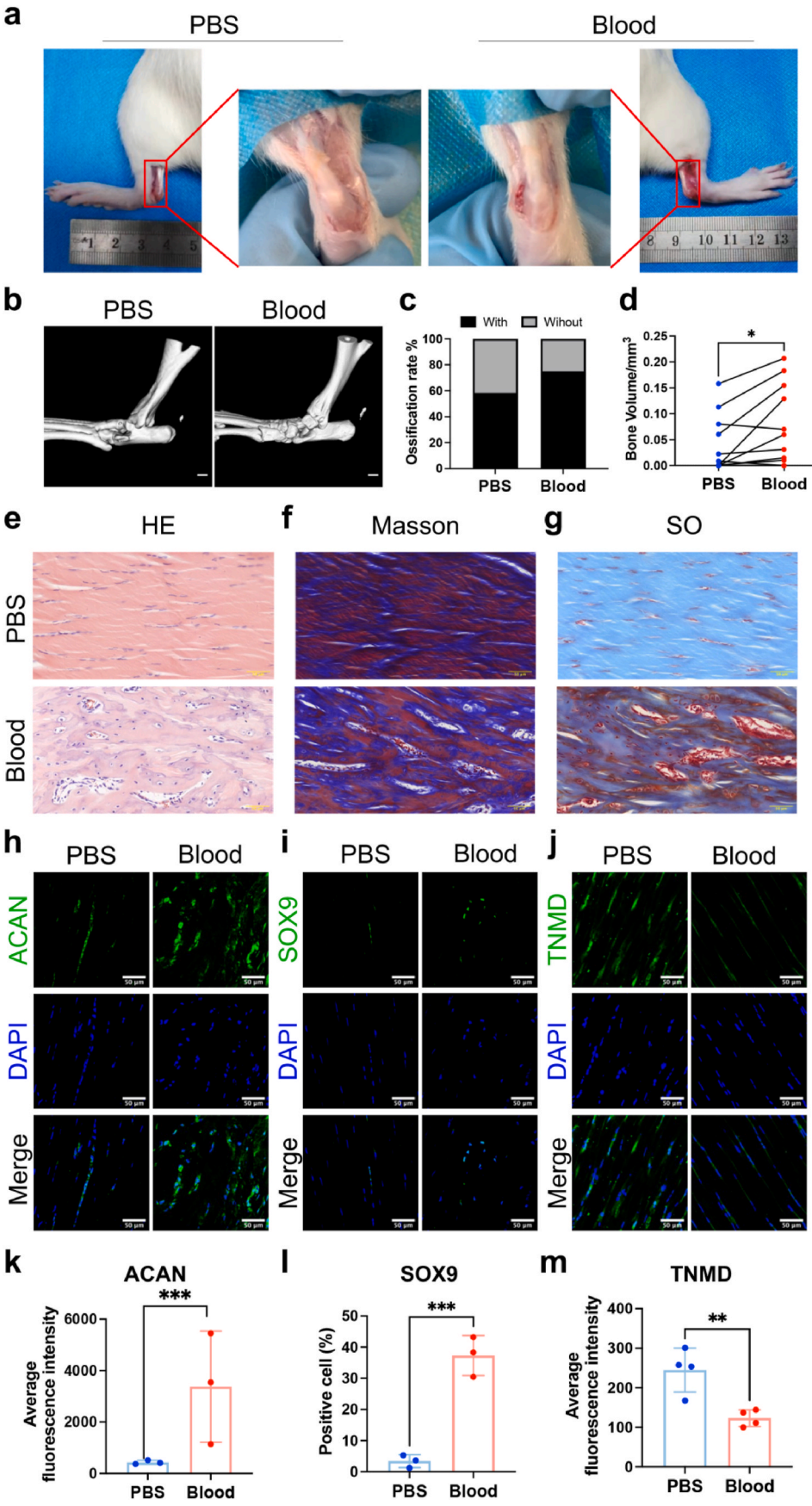

(caption on next page)

Fig. 2. Blood infiltration aggravated HO of the injured tendon in the long term. (a) Gross appearance of the Achilles tendon in the PBS and Blood groups on week 6. (b) Micro-CT imaging of the tendon in the PBS and Blood groups. Scale bar = 1 mm. (c) The ratio of heterotopic ossification of the injured tendon 6 weeks after surgery. (d) Quantitative analysis of the heterotopic bone volumes of the Achilles tendons in the PBS and Blood groups (n = 12, paired t-test, *P < 0.05). (e–g) HE, Masson, and SO staining of the tendon in the PBS and Blood groups. (h, k) Immunofluorescence staining and quantitative analysis of ACAN (n = 3, unpaired t-test, ***P < 0.001). Scale bar = 50 μm. (i, l) Immunofluorescence staining and quantitative analysis of SOX9 (n = 3, unpaired t-test, ***P < 0.001). Scale bar = 50 μm. (j, m) Immunofluorescence staining and quantitative analysis of TNMD (n = 4, unpaired t-test, ***P < 0.001). Scale bar = 50 μm.

from GO analysis were divided into three levels, Biological Process (BP), Cellular Component (CC), and Molecular Function (MF) (Fig. 5d). The processes of ossification and response to wounding were enriched in the BP category, consistent with our *in vivo* and *in vitro* results, demonstrating that blood treatment could promote tendon ossification and enhance the immune response. The enrichment results of CC showed that more DEGs were related to the extracellular matrix, especially collagen-containing extracellular matrix. In the MF category, most DEGs were enriched in binding and cell communication. These could explain the decrease of cell adhesion *in vitro*. In KEGG analysis, the PI3K/AKT signaling pathway was significantly upregulated (Fig. 5e). PI3K/AKT pathway would activate mTOR which was related to heterotopic ossification of tendon [25]. Then we performed GSEA analysis and found that the PI3K/AKT signaling pathway was also enriched in GSEA (Fig. 5f). The GSEA enrichment analysis of the PI3K/AKT signaling pathway showed relatively many significantly up-regulated genes in this pathway (Fig. 5g).

The PI3K/AKT/MTOR signaling pathway highlighted by GSEA analysis was using a mouse hallmark signaling pathway database. Results showed that most genes were upregulated in the blood treatment group (Fig. S3a). Moreover, we analyzed the relevant genes about adhesion, apoptosis, chondrogenesis, and tenogenesis, which were basically consistent with the results *in vitro* (Fig. S3b). Some genes (like Bcl2 and Scx) showed discrepancies that could be explained by a different microenvironment surrounding the TSPCs *in vitro* and *ex vivo*. Next, Cytoscape and Enrichment Map were used for visualization of the GSEA results as a network of enriched gene sets [31]. Integrin surface interaction and assembly collagen formation were significantly downregulated, which might be related to cell adhesion and tendon phenotype of TSPCs (Fig. S3c). The CNET plot showed the relationship between different signaling pathways enriched in KEGG and their shared genes (Fig. S3d). Next, Western blot analysis of tendon tissue showed that the PI3K/AKT pathway was activated in the blood treatment group compared to the PBS control group (Figs. S4a and b).

Therefore, transcriptome analysis suggested that the PI3K/AKT pathway was a potential mechanism for blood infiltration of tendons.

2.6. LY294002 inhibited the aberrant differentiation of blood-treated TSPCs by inhibiting the activation of the PI3K/AKT signaling pathway

To inhibit the aberrant differentiation of TSPCs induced by whole blood, we attempted to intervene in this process using small molecule compounds. Based on the results of the sequencing data and previous studies, we decided to choose LY294002, a small molecule inhibitor targeting PI3K, for further study. First, we screened the optimal concentration of LY294002 to avoid the potentially detrimental effects of too high the concentration on TSPCs activity, or too low the concentration to not achieve the desired inhibitory effect. We found that the IC50 of LY294002 in TSPCs was 32.53 μM (Fig. S5). It has been reported that 20 μM LY294002 can inhibit the abnormal differentiation of TSPCs [32]. Therefore, we selected 20 μM as the concentration of LY294002 in further experiments.

After blood treatment for different time (0, 6, 12, and 24 h), LY294002 was added into the fresh medium for cell culture. After 7 days, cells were collected to detect the expression of differentiation-related genes (Fig. 6a). As a result, LY294002 significantly inhibited the expression of Sox9, Runx2, and Col1A1. In addition, LY294002 could inhibit the expression of Scx and Mkx within a short period of blood treatment, but it had no significant inhibitory effects after prolonged blood treatment. In conclusion, LY294002 could significantly inhibit the osteochondrogenic gene expression of TSPCs, which confirmed the inhibitory effect of LY294002 on the abnormal differentiation of tendon stem cells caused by blood treatment.

Subsequently, after 7 days of culture, total cellular proteins were collected for western blotting analysis. The results displayed that phosphorylation of PI3K was inhibited. Furthermore, the expression of SOX9 was also downregulated (Fig. 6b, c). These results thus suggested that LY294002 could reduce the increase of SOX9 expression relevant to blood treatment via inhibition of PI3K/AKT signaling pathway activation. Finally, we found that LY294002 also decreased the ALP activity of TSPCs (Fig. 6d and e). All the above results proved the inhibitory effect of LY294002 on the osteochondrogenic differentiation of TSPCs.

2.7. LY294002 alleviated blood-induced tendon HO

We next investigated whether the inhibition of PI3K/AKT signaling pathway would attenuate HO progression. We then treated the blood-induced HO model rats with LY294002 or vehicle. Each rat received a subcutaneous injection (between the Achilles tendon and skin) of LY294002 or vehicle three times a week for three weeks from the third day after injury and was sacrificed at 6 weeks postinjury (Fig. 7a). Micro-CT showed that the HO formation and bone volume were significantly reduced in the LY294002-treated group compared with the control group at 6 weeks (Fig. 7b). Considering that trauma could also lead to HO formation, we performed an experiment with the PI3K/AKT inhibitor LY294002 intervention in an injured tendon model without blood injection and found that LY294002 treatment slightly reduced HO formation but was not statistically significant (Fig. S6). This implied that LY294002 was more meaningful for the blood-induced HO model due to the upregulation of the PI3K/AKT pathway. The succeeding experiments further characterized in detail the effect of LY294002 on blood-induced HO. Firstly, histological staining, including HE, Masson, and SO staining, identified a significant improvement in the LY294002-treated group. Importantly, little or no ectopic bone tissue was observed following LY294002 treatment (Fig. 7d–f). Protein levels of PI3K, p-PI3K, AKT, and p-AKT in tendon tissue were detected by Western blot (Fig. 7g and h). Results confirmed the inhibition of PI3K/AKT pathway. Overall, these results demonstrated that the inhibition of PI3K/AKT pathway with the small molecule LY294002 attenuated HO progression (see Fig. 8).

3. Discussion

In this study, we found that blood infiltration would induce acute inflammation and exacerbate heterotopic ossification of the injured tendon. And aberrant differentiation of TSPCs played a dominant role through the PI3K/AKT pathway. Afterward, we applied PI3K/AKT pathway inhibitor LY294002 to reverse the side effects of blood treatment. This is the first study focusing on the role of blood infiltration on the formation of HO of the injured tendon and the aberrant differentiation of TSPCs.

The effects of whole blood on the musculoskeletal system, such as hemophilic arthropathy, have been studied for a long time. Blood infiltration in the joints can lead to severe inflammation and chondrocyte apoptosis [33,34], and vascularization after bleeding often contributes to cartilage deterioration [35]. Since healthy cartilage and

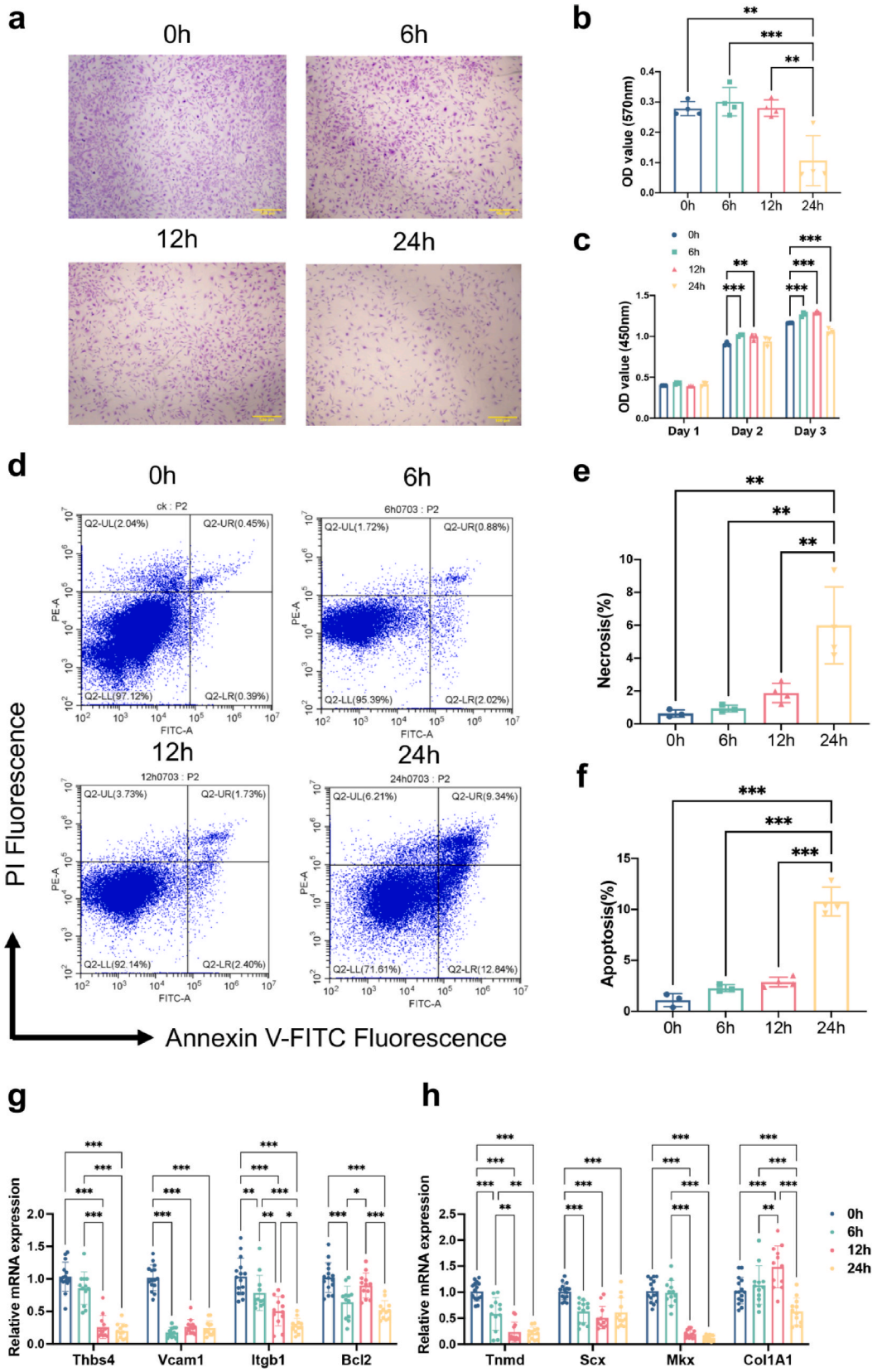

Fig. 3. Blood treatment increases cell apoptosis and decreases cell adhesion and tenonic gene expression. (a, b) Representative pictures and quantitative analysis of cell adhesion (n = 4, one-way ANOVA, **P < 0.01, ***P < 0.001). (c) Cell proliferation assay (n = 3, one-way ANOVA,**P < 0.01, ***P < 0.001). (d–f) Flow cytometric analysis of apoptosis and quantitative analysis of the percentages of necrotic cells and apoptotic cells (n = 4, one-way ANOVA, **P < 0.01, ***P < 0.001). (g) RT-qPCR of Thbs4, Vcam1, Itgb1, and Bcl2 expression (n = 15 in 0 h, n = 12 in 6, 12, and 24 h, one-way ANOVA, *P < 0.05, **P < 0.01, ***P < 0.001). (h) RT-qPCR of Tnmd, Scx, Mkx, and Col1A1 expression (n = 15 in 0 h, n = 12 in 6, 12, and 24 h, one-way ANOVA, **P < 0.01, ***P < 0.001).

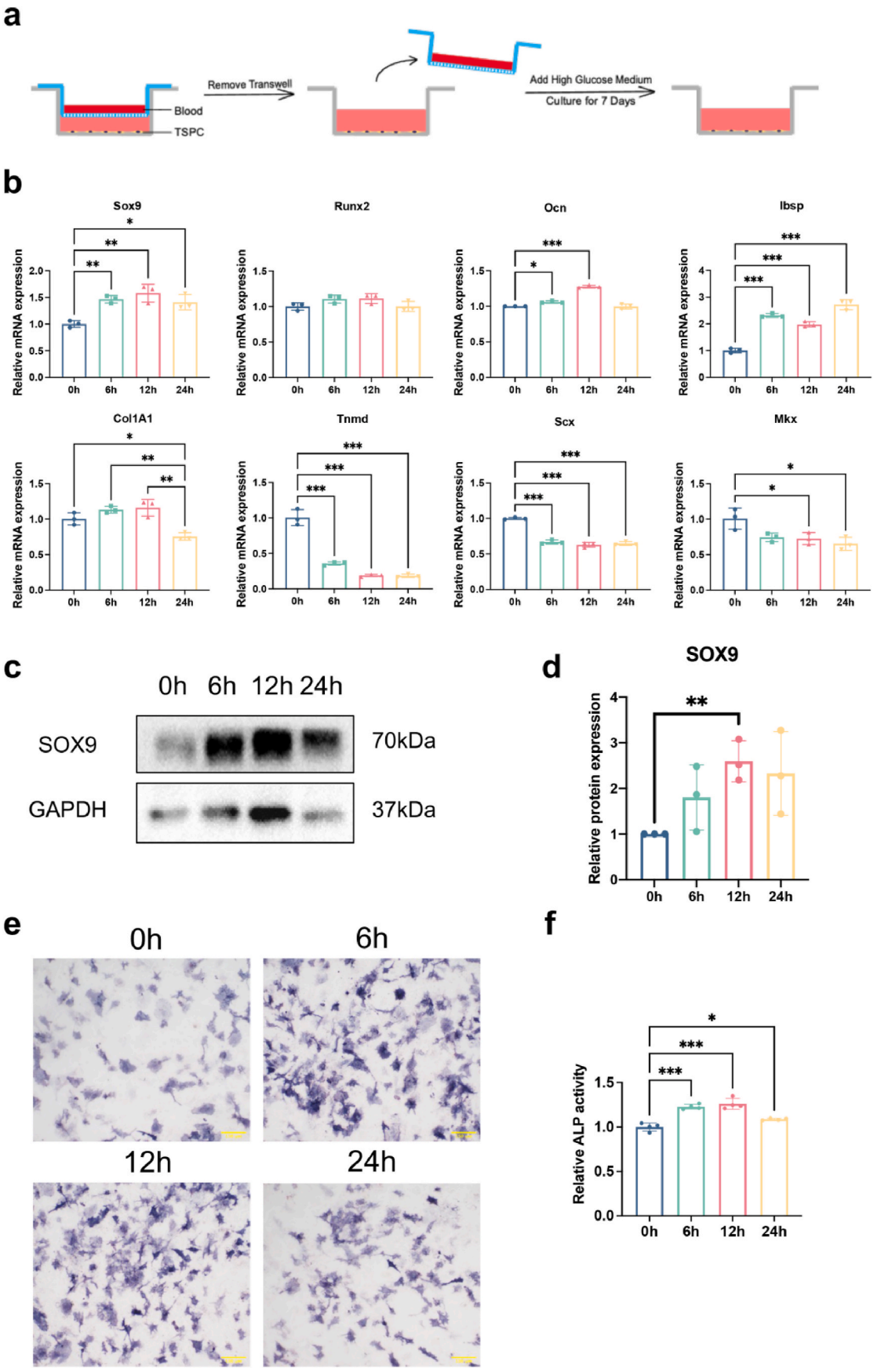

Fig. 4. Blood treatment induced aberrant differentiation of TSPCs. (a) Diagrammatic sketch. (b) RT-qPCR of Sox9, Runx2, Ocn, Ibsp, Col1A1, Tnmd, Scx, and Mkx expression (n = 3, one-way ANOVA, *P < 0.05, **P < 0.01, ***P < 0.001). (c, d) Western blot images and quantitative analysis of protein expression of SOX9 (n = 3, one-way ANOVA, **P < 0.01). (e, f) ALP staining and quantitative analysis of TSPCs (n = 4, one-way ANOVA, *P < 0.05, ***P < 0.001). Scale bar = 150 μm.

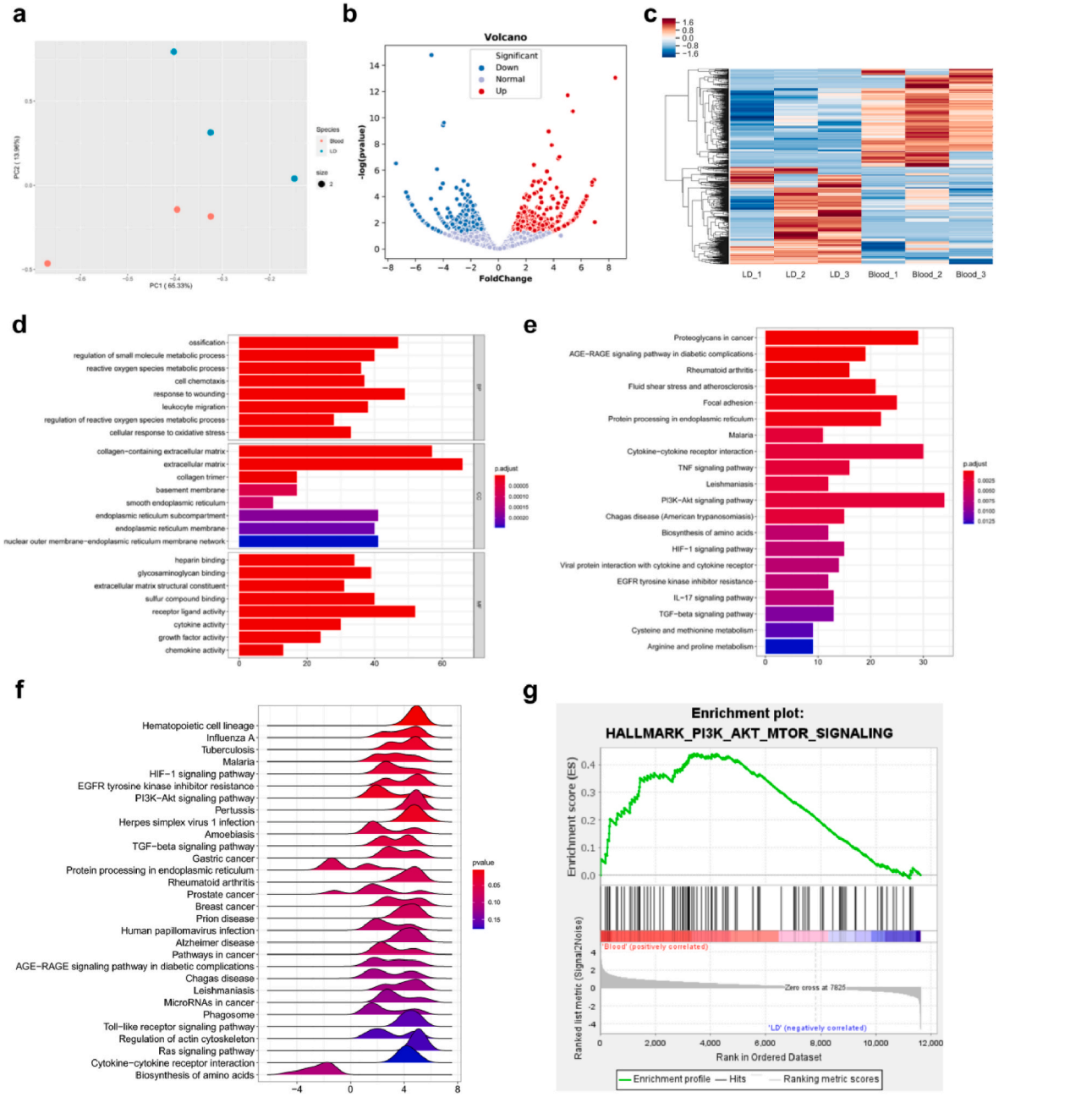

Fig. 5. Blood affects gene expression of the tendon tissues using transcriptional sequencing. (a) PCA analysis. (b) Volcano plot shows downregulated genes and upregulated genes. (c) Heatmaps of differential gene expression based on RNA-seq analysis. (d) GO analysis of DEGs (including Biological Process, Molecular Function, and Cellular Compartment). (e) KEGG enriched signaling pathways. (f) GSEA enriched pathways. (g) GSEA plot of PI3K/AKT signaling pathway.

tendons are both sparsely vascularized [36,37], we explored the short-term and long-term effects of blood on tendon considering the effects of blood on cartilage during inflammation and apoptosis. It was readily observed acute inflammation in the injured tendon, accompanied by macrophages aggregation and tendon matrix degeneration after blood injection on 3 days. The blood contains a large number of inflammatory mediators, and the injured tendon is stimulated by inflammatory mediators in the blood, which further recruits macrophages into the injured site [38]. The severe degeneration of the tendon matrix may be caused by the phagocytosis of recruited macrophages [39]. The previous study showed that the degree and duration of inflammation were closely related to tendon HO [40], consistent with our results that blood injection aggravated the HO of the injured tendon. It is generally believed that tendon HO is formed via endochondral ossification [10, 41]. Our work found that part of the tendon matrix was replaced by cartilage matrix, and chondrocytes-like cells appeared in the blood injection group.

TSPCs are important cell groups in maintaining tendon homeostasis. Blood infiltration would impair the TSPCs niche, while natural ordered collagenous matrices could support TSPCs adhesion and proliferation [42]. We found that short-term blood contact could stimulate the proliferation of TSPCs. But 24 h blood treatment inhibited cell proliferation and adhesion. The reduced proliferation ability of TSPCs might reduce the amount of TSPC available for tendon repair after injury and might contribute to failed tendon healing such as HO [43]. Moreover, apoptosis is an important part of cell proliferation control and maintaining cell homeostasis, and increased apoptosis of TSPCs is the basic mechanism leading to tendon diseases [44]. We also found that

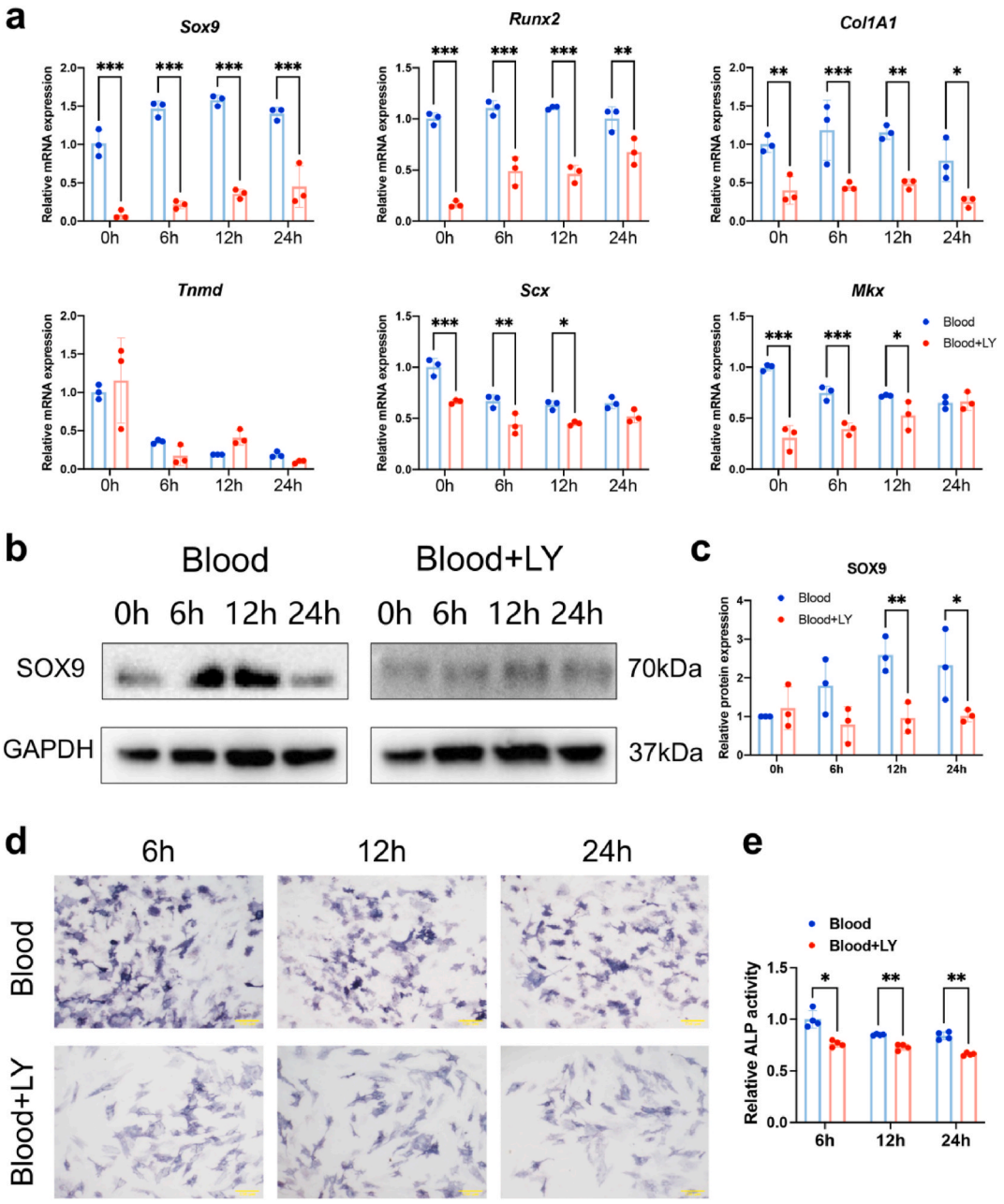

Fig. 6. LY294002 inhibited the aberrant differentiation of blood-treated TSPCs by inhibiting the activation of the PI3K/AKT signaling pathway. (a) RT-qPCR of Sox9, Runx2, Col1A1, Tnmd, Scx, and Mkx expression (n = 3, one-way ANOVA, *P < 0.05, **P < 0.01, ***P < 0.001). (b, c) Western blot images and quantitative analysis of protein expression of SOX9 after LY294002 treatment (n = 3, one-way ANOVA, *P < 0.05, **P < 0.01). (d, e) ALP staining and quantitative analysis of TSPCs (n = 4, one-way ANOVA, *P < 0.05, **P < 0.01). Scale bar = 150 μm.

apoptosis of TSPCs increased in a time-dependent manner, which might weaken tendon regeneration ability. Besides, blood reduced the tenonic genes expression of TSPCs. Tnmd is the best-known mature marker for tendon lineage cells, which is of great significance for tendon maturation and the resident TSPCs [45]. We observed that the expression of Tnmd in the tendon tissue of the blood injection group significantly decreased in 6 weeks. This reflected that blood infiltration would disrupt the maintenance of tendon homeostasis. Aberrant differentiation of TSPCs into osteochondral tissue is associated with the pathogenesis of chronic tenopathy [43]. To explore the biological mechanism in depth, we investigated the role of differentiation directions of TSPCs in tendon HO. In a collagenase-induced tendon injury model, TSPCs showed a changed fate, with higher osteogenic and chondrogenic differentiation potential, but lower tendon differentiation ability and lower proliferation ability [43]. Our study also demonstrated that blood could induce TSPCs to differentiate in the wrong direction (endochondral ossification).

The mechanisms underlying the pathogenesis of tendon HO caused by blood remain unclear. Here, the transcriptome sequencing method was used to analyse the tendon tissues of mice treated with whole blood, and the mechanisms of HO of the injured tendon induced by whole blood were delineated to a certain extent. Transcriptome sequencing results showed that PI3K/AKT pathways were highly active in blood treatment groups. Previous studies have shown that PI3K/AKT pathway is related to ectopic ossification and inhibiting PI3K can prevent ectopic ossification [32,46]. Aspirin could inhibit adipogenesis of TSPCs and fatty infiltration of the injured tendon by downregulating PTEN/PI3-K/AKT signaling to promote tendon repair [47]. In addition, PI3K/AKT axis also integrates other additional major osteogenic signaling

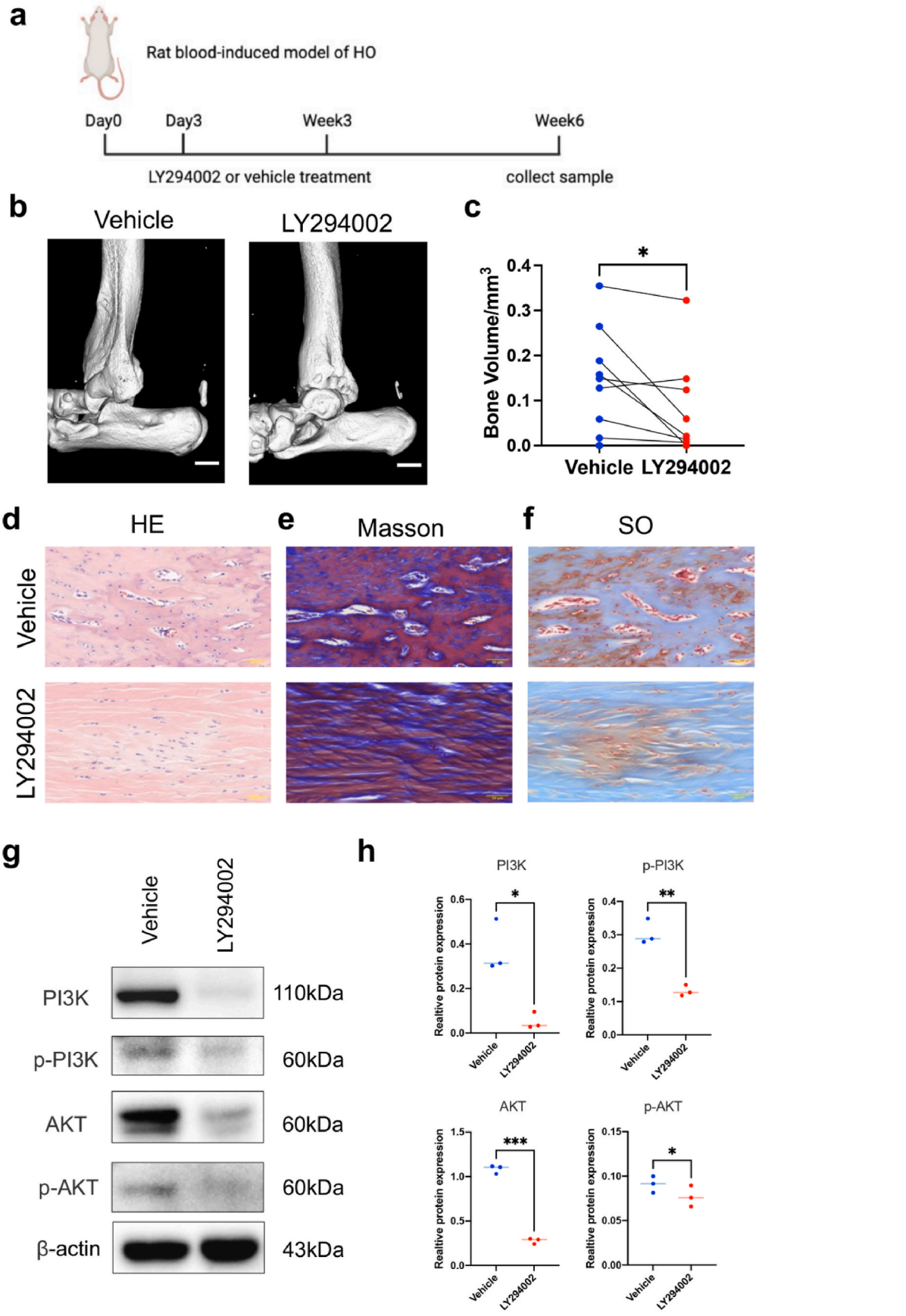

(caption on next page)

Fig. 7. LY294002 alleviates blood-induced tendon HO. (a) Schematic illustration of the treatment and sample collection workflow for the rat HO model. (b, c) Micro-CT imaging and quantitative analysis of the tendon in the LY294002 treatment and vehicle treatment groups (n = 13, paired t-test, *P < 0.05). Scale bar = 1 mm. (d–f) HE, Masson, and SO staining of the tendon in the LY294002 treatment and vehicle treatment groups. (g, h) Western blot images and quantitative analysis of protein expression of PI3K, p-PI3K, AKT, and p-AKT of the tendon in the LY294002 treatment and vehicle treatment groups (n = 3, unpaired t-test, *P < 0.05, **P < 0.01, ***P < 0.001).

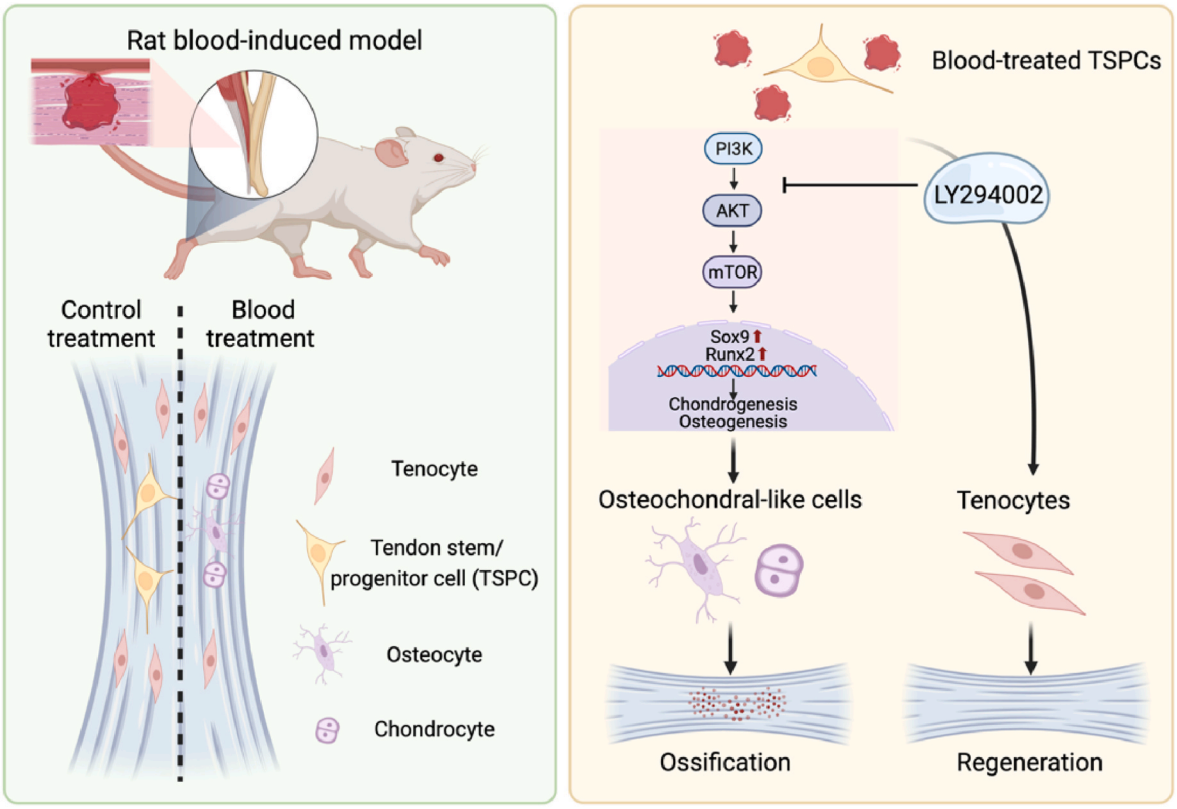

Fig. 8. Schematic diagram of the role of the blood on the heterotopic ossification of the injured tendon.

pathways such as mTOR while rapamycin (mTOR inhibitor) can significantly treat tendon HO [25,48,49]. Accordingly, we evaluated the feasibility and effectiveness of the small molecule drug LY294002 in targeting the PI3K/AKT signaling pathway. Surprisingly, we proved that LY294002 partially circumvented this osteochondrogenic tendency of blood-treated TSPCs. All these provided the new therapeutic potential of PI3K/AKT inhibitor in treating tendon injury and tendinopathy.

In conclusion, our findings indicate that blood infiltration will exacerbate tendon HO, relying on aberrant differentiation of TSPCs via PI3K/AKT signaling pathway. These will provide new insights into the pathology of tendon injury and clues to block the pathological process and initiate regeneration.

4. Materials and methods

4.1. Animal experiments

Thirty male adult Sprague–Dawley rats (8 weeks old, body weight 200–250 g, purchased from Shanghai SLAC Laboratory Animal Company, Shanghai, China) were used in this study.

Rats were anesthetized by pentobarbital sodium (40 mg/kg). A 27-gauge needle (B. Braun, Deutschland) was used to puncture the Achilles tendon body from the lateral aspect percutaneously, and this process was repeated at three different parts of the Achilles tendon body for each rat. Blood or PBS was injected at the same time as the puncture. Autologous whole blood from the caudal vein was injected as the treatment, and sterilized phosphate buffered saline (PBS) was injected into the other Achilles tendon as the control. The total injection volume was 100 μl.

During the feeding process, the rats were free to get water and food. The feeding temperature and humidity were kept constant. The rats were sacrificed at 3 days and 6 weeks after the injection. The Achilles tendons were collected for further experiments.

4.2. Micro-computed tomography (micro-CT) analysis

Micro-CT was used to scan the Achilles tendon, and Imalytics preclinical software was used for three-dimensional reconstruction to observe the formation of tendon HO in rats and analyse the volume of ossification.

4.3. Histology

The Achilles tendons were fixed with 4 % (w/v) paraformaldehyde (PFA) for 24 h at 4 °C and subsequently decalcified in 10 % (w/v) ethylenediaminetetraacetic acid disodium salt (EDTA) solution for 3–5 weeks. Then the tendon samples were paraffin-embedded and cut into 5 μm thick sections. Hematoxylin-eosin (HE), Masson's trichrome, and Safranin O staining were carried out following standard protocols [25]. A slide scanner (VS200, Olympus, Japan) was used to acquire digital micrographs.

4.4. Immunofluorescence staining

After gradient dewaxing, paraffin sections were soaked in the sodium citrate buffer solution at 65 °C overnight for antigen retrieval. The samples were then blocked with 5 % (w/v) bovine serum albumin (BSA) (Sango, China), and then incubated with the primary antibodies overnight at 4 °C. Corresponding fluorescence labeled secondary antibodies were added for 2 h at room temperature (RT). Cell nuclei were stained with DAPI (C1002, 1:1000, Beyotime, China). After washing with PBS, the sections were mounted with antifading mounting medium (S2100, Solarbio, China). Imaging was performed with an Olympus FV1000 confocal microscope. For quantification of fluorescence intensity, 6 random fields per section were considered. The antibodies were listed in Table 1.

4.5. Isolation and culture of TSPCs

Mouse TSPCs were isolated from tail tendons of 2-week-old C57 wildtype mice. Tail tendons were digested with 0.2 % type I collagenase (17100017, Invitrogen, USA) at 37 °C for 4–6 h to obtain isolated cells. TSPCs were cultured in low glucose Dulbecco's modified Eagle's medium (L-DMEM) (Gibco, USA) supplemented with 10 % (v/v) fetal bovine serum (FBS) and 1 % (v/v) penicillin/streptomycin solution at 37 °C and 5 % CO_2. Routine passages were carried out when cell culture reached 80 % confluence. Cells at passage 1–2 were used for further experiments.

4.6. Blood treatment of TSPCs

The TSPCs were allowed to adhere and culture for 24 h, and then a blood-containing medium in transwells was added. After blood treatment for 0, 6, 12, or 24 h, the transwells were removed and the medium was changed to normal medium or differentiation medium according to subsequent experiments. The medium was changed every 2–3 days.

Table 1
Antibody list.

Primary antibodies		
Name	Source	Application
CD18-PE	Biolegend, 101,407	1:50(Flow Cyt)
CD34-PE	Biolegend, 119,307	1:100(Flow Cyt)
CD44-APC	Biolegend, 103,011	1:100(Flow Cyt)
CD45-PE	Biolegend, 103,105	1:100(Flow Cyt)
CD90.2-PE	eBioscience, 12-0902-81	1:100(Flow Cyt)
Sca-1-FITC	Abcam, ab25031	1:100(Flow Cyt)
Rabbit anti-SOX9	Abcam, ab185966	1:1000 (IF), 1:1000 (WB)
Mouse anti-CD68	Abcam, ab53444	1:1000 (IF)
Rabbit anti-ACAN	Abcam, ab36861	1:1000 (IF)
Rabbit anti-TNMD	Abcam, ab203676	1:100 (IF)
Rabbit anti-PI3K	Cell Signaling Technology, 4249	1:1000 (WB)
Rabbit anti-phospho-PI3K	Cell Signaling Technology, 17,366	1:1000 (WB)
Rabbit anti-AKT	Cell Signaling Technology, 4691	1:1000 (WB)
Rabbit anti-phpspho-AKT	Cell Signaling Technology, 4060	1:1000 (WB)
Rabbit anti-GAPDH	Cell Signaling Technology, 5174	1:1000 (WB)
Mouse anti-β-actin	Immunoway, YM3028	1:1000 (WB)
Secondary antibodies		
Name	**Source**	**Application**
Goat anti-rabbit 488	Invitrogen, A11008	1:1000 (IF)
Goat anti-mouse 488	Invitrogen, A21202	1:1000 (IF)
Goat anti-rabbit HRP	Jackson, 111-035-003	1:6000 (WB)
Goat anti-mouse HRP	Jackson, 115-035-003	1:6000 (WB)

4.7. Flow cytometry analysis

TSPCs were harvested and blocked with 1 % BSA for 30 min at 4 °C. Subsequently, the cells were stained with fluorescein-conjugated antibodies for 30 min at 4 °C. The corresponding isotype antibodies were used as controls. The assay was performed by a flow cytometer (BD FACSCantoTM; BD Biosciences, USA) and analysed by FlowJo v10 software. The antibodies were listed in Table 1.

4.8. Osteogenic differentiation assay

Osteogenic differentiation medium comprised High glucose DMEM (H-DMEM; Gibco, USA) supplemented with 10 % FBS, 0.1 μM dexamethasone (Sigma, USA), 50 μM ascorbic acid (Sigma, USA), and 10 mM β-glycerol phosphate (Sigma, USA). On day 7, the alkaline phosphatase (ALP) activity of TSPCs was evaluated via a kit (C3206, Beyotime, China). On day 14, the calcium-rich extracellular matrix of TSPCs was stained by 2 % Alizarin Red (ARS) solutions (Sigma, USA).

4.9. Chondrogenic differentiation assay

Chondrogenic differentiation medium comprised H-DMEM, 1 % sodium pyruvate (Gibco, USA), 1 % Insulin-Transferrin-Selenium (Gibco, USA), 100 nM dexamethasone (Sigma, USA), 50 μg/ml L-ascorbic acid (Sigma, USA) and 10 ng/ml TGF-β3 (Novoprotein, China). On day 14, the production of GAG was measured by Alcian blue (Sigma, USA) staining.

4.10. Adipogenic differentiation assay

Adipogenic differentiation medium comprised H-DMEM, 10 % FBS, 1 μM dexamethasone (Sigma, USA), 500 μM 3-isobutyl-1-methylxanthine (IBMX; Sigma, USA), and 200 μM indomethacin (Sigma, USA). On day 14, the production of oil droplets was measured by Oil red (Sigma, USA) staining.

4.11. Colony formation unit assay

TSPCs were harvested and seeded at a density of 80 cells/cm^2, followed by culturing for 10 days. Cells were fixed with 4 % PFA and then stained with 0.1 % (w/v) crystal violet methanol solution at RT for 20 min. After removing float dyestuff, the clone formation was observed under the microscope.

4.12. Blood treatment of tendon tissues ex vivo

Achilles tendons obtained from 8-week-old C57 wildtype mice were used for *ex vivo* culture. Firstly, the tendon tissues were washed with PBS supplemented with 1 % (v/v) PS. And then the tendon tissues were cultured in L-DMEM supplemented with 20 % (v/v) mouse anticoagulant whole blood. After 3 days, tendon tissues were washed with PBS and the RNA was extracted for sequencing.

4.13. Cell adhesion assay

TSPCs were harvested and adhered to the dish for 3 h, followed by crystal violet staining. For quantitative analysis, 33 % (v/v) acetic acid was added to each well. Supernatants were used for obtaining optical density (OD) values of the dye by measuring the absorbance at 570 nm.

4.14. Cell proliferation assay

Cell proliferation was monitored by CCK-8 (CCK-8; Dojindo, Japan). Briefly, the CCK-8 solution was added into the culture medium at 1:10. Absorbance at 450 nm was measured after 2 h of incubation.

4.15. Detection of apoptosis

Annexin V-FITC Apoptosis Detection Kit (Beyotime, China) was used to detect apoptosis by flow cytometry and fluorescence microscopy. Briefly, cells were harvested by trypsin digestion and then collected with culture medium to prevent the loss of suspension cells. Samples were washed with PBS, resuspended in detection solution, and incubated for 10 min at RT. The fluorescence was observed under an Olympus FV1000 confocal microscope. The ratio of apoptosis and necrosis was measured by the Cytoflex flow cytometer (Beckman Coulter, USA), and analysed by FlowJo v10 software.

4.16. Real-time quantitative PCR

Total RNA from TSPCs was extracted by TRIzol reagent (Invitrogen, USA), and cDNA was obtained using a reverse transcription kit (Toyobo, Japan). The RNA levels were quantified by real-time PCR with TB Green Premix Ex Taq (TaKaRa, Japan). Fluorescence quantification analysis was carried out by a high throughput fluorescent quantitative PCR instrument (Roche, Deutschland). The primers were shown in Table 2.

4.17. RNA sequencing (RNA-seq) analysis

RNA was extracted from *ex vivo* tendon tissues and sequenced on Illumina X-Ten platform following a previous method [50]. Both the blood treatment group and control group contained three replicates. Sequence reads were aligned to the reference genome (mm10) using HISAT2 [51] and SAMtools [52], and gene counts were calculated using HTSeq [53]. Statistical analysis and result visualization were performed by R language and Python. We used EBSeq [54] to identify differentially expressed genes (DEGs), and clusterProfiler [55] to enrich pathways to show the results of the KEGG, GO and GSEA analysis. DEGs were defined as genes with foldchange $\geq$2 and p-value $\leq$0.05. Heatmap and volcano plots were drawn using seaborn in Python. KEGG, GO, GSEA, and CNET plots were drawn using ggplot2 in R. Then, we used CMap [56] to look for inhibitors of enrichment pathways.

Table 2
Primer sequences for RT-qPCR.

Primer Name	Base sequence
Mouse-THBS4-F	ACGGCTGAACAAAGCCATC
Mouse-THBS4-R	TTGCTCAGTCTCAGGAGAACC
Mouse-VCAM1-F	CTTCCAGAACCCTTCTCAG
Mouse-VCAM1-R	GGGACCATTCCAGTCACACTTC
Mouse-ITGB1-F	CTACTGGTCCCGACATCATCC
Mouse-ITGB1-R	TGACCACAGTTGTCACGGCAC
Mouse-SOX9-F	GAGCCGGATCTGAAGAGGGA
Mouse-SOX9-R	GCTTGACGTGTGGCTTGTTC
Mouse-RUNX2-F	CGGTCTCCTTCAGGATGGT
Mouse-RUNX2-R	GCTTCCGTCAGCGTCAACA
Mouse-BCL2-F	GGATAACGGAGGCTGGGATGCCT
Mouse-BCL2-R	TTGTCGACCTCACTTGTGGCCC
Mouse-COL1A1-F	GCTCCTCTTAGGGGCCACT
Mouse-COL1A1-R	CCACGTCTCACCATTGGGG
Mouse-TNMD-F	ACACTTCTGGCCCGAGGTAT
Mouse-TNMD-R	GACTTCCAATGTTTCATCAGTGC
Mouse-SCX-F	CCTTCTGCCTCAGCAACCAG
Mouse-SCX-R	GGTCCAAAGTGGGGCTCTCCGTGACT
Mouse-MKX-F	CCCCGGACATCGGATCTACTA
Mouse-MKX-R	CTCTTAGGATGAGGATTTAGGTA
Mouse–OCN–F	GACCATCTTTCTGCTCACTCTG
Mouse–OCN–R	TACCTTATTGCCCTCCTGCTTG
Mouse-IBSP-F	CGGCACTCCAACTGCCCAAGA
Mouse-IBSP-R	TGCCATTCCCGCCATCCACC
Mouse-GAPDH-F	ATACGGCTACAGCAACAGGG
Mouse-GAPDH-R	TGTGAGGGAGATGCTCAGTG
Rat-IL1β-F	GCCCGTCCTCTGTGACTCGT
Rat-IL1β-R	TGTCGTTGCTTGTCTCTCCTTGTA
Rat-IL10-F	CAGCTGCGACGCTGTCATCG
Rat-IL10-R	GCAGTCCAGTAGATGCCGGGT
Rat-MMP9-F	GCAGGGCCCCTTTCTTATTG
Rat-MMP9-R	CTGGCCTGTGTACACCCACA
Rat-GAPDH-F	GCAAGTTCAACGGCACAG
Rat-GAPDH-R	GCCAGTAGACTCCACGACA

4.18. Western blot analysis

We performed western blot to quantify the changes in cell protein expression level after blood treatment. TSPCs were digested with trypsin and collected. Then RIPA lysis buffer (Beyotime, China) was applied to lyse cells to obtain whole cell protein extracts. Protein samples were separated by 8 % (w/v) sodium dodecyl sulfate-polyacrylamide gel electrophoresis (SDS-PAGE) and transferred onto a PVDF membrane (Millipore, USA). The membranes were blocked in blocking solution (Beyotime, China) at RT for 2 h and then incubated with primary antibodies at 4 °C overnight. Later, the membranes were washed three times with Tris buffer saline with Tween 20 (TBST) and continued to be incubated with the secondary antibodies at RT for 2 h. At last, the membranes were developed with enhanced chemiluminescence (ECL) kit (Beyotime, China). The antibodies were listed in Table 1.

4.19. Statistical analysis

Data were tested for homogeneity of variances and normality. Homogeneity of variances was estimated with the Levene test. Data normality was tested using Shapiro–Wilk normality test and the D'Agostino-Pearson omnibus test. The data were presented as means ± standard deviations (SD). Analyses of statistically significant differences between data sets were performed using Student's t-test or an ANOVA test where appropriate. Paired t-test was used to compare continuous parameters of the bilateral tendon from the same animal, and other continuous parameters were compared by an unpaired t-test. For one-way ANOVA, post-hoc analysis with Tukey multiple comparison was used for controlling the family-wise error rate. Statistical significance is denoted as below: ns (indicating no statistical significance), *$p < 0.05$, **$p < 0.01$, ***$p < 0.001$. Statistical analysis was performed using GraphPad Prism 9.

Author contributions

Conceptualisation, X.C., Y.Y., J.Z., and H.O.; Methodology, X.C., Y. Y., Y.G., J.Y., W.Y., Z.S., Y.Z., J.W., F.B., Y.W., Z.W., Y.X., C.G.; Writing-original draft, X.C. and Y.Y.; Writing review & editing, B.H., H.W., J.Z., and H.O.; Supervision, H.L., Z.Y., X.C. J.Z., and H.O.; Funding acquisition, J.Z. and H.O.

Ethical approval

All animal procedures were approved by the Zhejiang University Institutional Animal Care and Use Committee (ZJU20200113).

Consent for publication

Not applicable.

Funding

This work was supported by the National Key Research and Development Program of China (2023YFB3813000), the National Natural Science Foundation of China (T2121004, 31830029), Zhejiang Provincial Natural Science Foundation of China (LTGY23H060009) and Huzhou Hospital of Zhejiang University School of Medicine-School of Basic Medicine of Zhejiang University Joint Research Grant.

Declaration of competing interest

The authors declare no competing financial interests.

Acknowledgments

The authors thank Shuangshuang Liu from the Core Facilities, Zhejiang University School of Medicine for technical assistance.

Appendix A. Supplementary data

Supplementary data to this article can be found online at https://doi.org/10.1016/j.jot.2023.11.003.

References

[1] Maffulli N. Autologous blood products in musculoskeletal medicine. BMJ 2013;346:f2979. https://doi.org/10.1136/bmj.f2979.
[2] van der Bijl I, Vlig M, Middelkoop E, de Korte D. Allogeneic platelet-rich plasma (PRP) is superior to platelets or plasma alone in stimulating fibroblast proliferation and migration, angiogenesis, and chemotaxis as relevant processes for wound healing. Transfusion 2019;59(11):3492–500. https://doi.org/10.1111/trf.15535.
[3] Scully D, Sfyri P, Verpoorten S, Papadopoulos P, Muñoz-Turrillas MC, Mitchell R, et al. Platelet releasate promotes skeletal myogenesis by increasing muscle stem cell commitment to differentiation and accelerates muscle regeneration following acute injury. Acta Physiol 2019;225(3):e13207. https://doi.org/10.1111/apha.13207.
[4] Bell KJ, Fulcher ML, Rowlands DS, Kerse N. Impact of autologous blood injections in treatment of mid-portion Achilles tendinopathy: double blind randomised controlled trial. BMJ 2013;346:f2310. https://doi.org/10.1136/bmj.f2310.
[5] Branson R, Naidu K, du Toit C, Rotstein AH, Kiss R, McMillan D, et al. Comparison of corticosteroid, autologous blood or sclerosant injections for chronic tennis elbow. J Sci Med Sport 2017;20(6):528–33. https://doi.org/10.1016/j.jsams.2016.10.010.
[6] Cruz-Montecinos C, Perez-Alenda S, Oyarzun-Tejeda A, Cerda M, Querol-Fuentes F. Estimation of tensile properties of the Achilles tendon in haemophilic arthropathy of the ankle: case study. Haemophilia 2015;21(2):e141–3. https://doi.org/10.1111/hae.12619.
[7] Docheva D, Müller SA, Majewski M, Evans CH. Biologics for tendon repair. Adv Drug Deliv Rev 2015;84:222–39. https://doi.org/10.1016/j.addr.2014.11.015.
[8] Bi Y, Ehirchiou D, Kilts TM, Inkson CA, Embree MC, Sonoyama W, et al. Identification of tendon stem/progenitor cells and the role of the extracellular matrix in their niche. Nat Med 2007;13(10):1219–27. https://doi.org/10.1038/nm1630.
[9] Hu JJ, Yin Z, Shen WL, Xie YB, Zhu T, Lu P, et al. Pharmacological regulation of in Situ tissue stem cells differentiation for Soft tissue calcification treatment. Stem Cell 2016;34(4):1083–96. https://doi.org/10.1002/stem.2306.
[10] Zhang Q, Zhou D, Wang H, Tan J. Heterotopic ossification of tendon and ligament. J Cell Mol Med 2020;24(10):5428–37. https://doi.org/10.1111/jcmm.15240.
[11] Steward AJ, Kelly DJ. Mechanical regulation of mesenchymal stem cell differentiation. J Anat 2015;227(6):717–31. https://doi.org/10.1111/joa.12243.
[12] Gulotta LV, Kovacevic D, Cordasco F, Rodeo SA. Evaluation of tumor necrosis factor α blockade on early tendon-to-bone healing in a rat rotator cuff repair model. Arthroscopy 2011;27(10):1351–7. https://doi.org/10.1016/j.arthro.2011.03.076.
[13] Huang Y, Wang X, Zhou D, Zhou W, Dai F, Lin H. Macrophages in heterotopic ossification: from mechanisms to therapy. NPJ Regen Med 2021;6(1):70. https://doi.org/10.1038/s41536-021-00178-4.
[14] Sorkin M, Huber AK, Hwang C, Carson WFt, Menon R, Li J, et al. Regulation of heterotopic ossification by monocytes in a mouse model of aberrant wound healing. Nat Commun 2020;11(1):722. https://doi.org/10.1038/s41467-019-14172-4.
[15] Li D, Jiang Y, He P, Li Y, Wu Y, Lei W, et al. Hypoxia drives material-induced heterotopic bone formation by enhancing osteoclastogenesis via M2/lipid-loaded macrophage Axis. Adv Sci 2023;10(15):e2207224. https://doi.org/10.1002/advs.202207224.
[16] Agarwal S, Loder SJ, Cholok D, Peterson J, Li J, Breuler C, et al. Scleraxis-lineage cells contribute to ectopic bone formation in muscle and tendon. Stem Cell 2017;35(3):705–10. https://doi.org/10.1002/stem.2515.
[17] Dey D, Bagarova J, Hatsell SJ, Armstrong KA, Huang L, Ermann J, et al. Two tissue-resident progenitor lineages drive distinct phenotypes of heterotopic ossification. Sci Transl Med 2016;8(366):366ra163. https://doi.org/10.1126/scitranslmed.aaf1090.
[18] Feng H, Xing W, Han Y, Sun J, Kong M, Gao B, et al. Tendon-derived cathepsin K-expressing progenitor cells activate Hedgehog signaling to drive heterotopic ossification. J Clin Invest 2020;130(12):6354–65. https://doi.org/10.1172/JCI132518.
[19] Kan C, Chen L, Hu Y, Ding N, Li Y, McGuire TL, et al. Gli1-labeled adult mesenchymal stem/progenitor cells and hedgehog signaling contribute to endochondral heterotopic ossification. Bone 2018;109:71–9. https://doi.org/10.1016/j.bone.2017.06.014.
[20] Olmsted-Davis EA, Salisbury EA, Hoang D, Davis EL, Lazard Z, Sonnet C, et al. Progenitors in peripheral nerves launch heterotopic ossification. Stem Cells Transl Med 2017;6(4):1109–19. https://doi.org/10.1002/sctm.16-0347.
[21] Klatte-Schulz F, Minkwitz S, Schmock A, Bormann N, Kurtoglu A, Tsitsilonis S, et al. Different Achilles tendon pathologies show distinct histological and molecular characteristics. Int J Mol Sci 2018;19(2). https://doi.org/10.3390/ijms19020404.
[22] Richards PJ, Braid JC, Carmont MR, Maffulli N. Achilles tendon ossification: pathology, imaging and aetiology. Disabil Rehabil 2008;30(20–22):1651–65. https://doi.org/10.1080/09638280701785866.
[23] Chen M, Xiao L, Dai G, Lu P, Zhang Y, Li Y, et al. Inhibition of JAK-STAT signaling pathway alleviates age-related phenotypes in tendon stem/progenitor cells. Front Cell Dev Biol 2021;9:650250. https://doi.org/10.3389/fcell.2021.650250.
[24] Magne D, Bougault C. What understanding tendon cell differentiation can teach us about pathological tendon ossification. Histol Histopathol 2015;30(8):901–10. https://doi.org/10.14670/HH-11-614.
[25] Chen Y, Shen W, Tang C, Huang J, Fan C, Yin Z, et al. Targeted pathological collagen delivery of sustained-release rapamycin to prevent heterotopic ossification. Sci Adv 2020;6(18):eaay9526. https://doi.org/10.1126/sciadv.aay9526.
[26] Alenzi FQ. Links between apoptosis, proliferation and the cell cycle. Br J Biomed Sci 2004;61(2):99–102. https://doi.org/10.1080/09674845.2004.11732652.
[27] Hata AN, Engelman JA, Faber AC. The BCL2 family: key mediators of the apoptotic response to targeted anticancer therapeutics. Cancer Discov 2015;5(5):475–87. https://doi.org/10.1158/2159-8290.CD-15-0011.
[28] Ragni E, Perucca Orfei C, Bowles AC, de Girolamo L, Correa D. Reliable reference genes for gene expression assessment in tendon-derived cells under inflammatory and pro-fibrotic/healing Stimuli. Cells 2019;8(10). https://doi.org/10.3390/cells8101188.
[29] Asai S, Otsuru S, Candela ME, Cantley L, Uchibe K, Hofmann TJ, et al. Tendon progenitor cells in injured tendons have strong chondrogenic potential: the CD105-negative subpopulation induces chondrogenic degeneration. Stem Cell 2014;32(12):3266–77. https://doi.org/10.1002/stem.1847.
[30] Tuzmen C, Verdelis K, Weiss L, Campbell P. Crosstalk between substance P and calcitonin gene-related peptide during heterotopic ossification in murine Achilles tendon. J Orthop Res 2018;36(5):1444–55. https://doi.org/10.1002/jor.23833.
[31] Reimand J, Isserlin R, Voisin V, Kucera M, Tannus-Lopes C, Rostamianfar A, et al. Pathway enrichment analysis and visualization of omics data using g:Profiler, GSEA, Cytoscape and EnrichmentMap. Nat Protoc 2019;14(2):482–517. https://doi.org/10.1038/s41596-018-0103-9.
[32] Liu J, Chen L, Tao X, Tang K. Phosphoinositide 3-kinase/Akt signaling is essential for prostaglandin E2-induced osteogenic differentiation of rat tendon stem cells. Biochem Biophys Res Commun 2013;435(4):514–9. https://doi.org/10.1016/j.bbrc.2012.11.083.
[33] Christensen KR, Kjelgaard-Hansen M, Nielsen LN, Wiinberg B, Alexander Althoehn F, Bloksgaard Poulsen N, et al. Rapid inflammation and early degeneration of bone and cartilage revealed in a time-course study of induced haemarthrosis in haemophilic rats. Rheumatology 2019;58(4):588–99. https://doi.org/10.1093/rheumatology/key186.
[34] Melchiorre D, Manetti M, Matucci-Cerinic M. Pathophysiology of hemophilic arthropathy. J Clin Med 2017;6(7). https://doi.org/10.3390/jcm6070063.
[35] Bhat V, Olmer M, Joshi S, Durden DL, Cramer TJ, Barnes RF, et al. Vascular remodeling underlies rebleeding in hemophilic arthropathy. Am J Hematol 2015;90(11):1027–35. https://doi.org/10.1002/ajh.24133.
[36] Mapp PI, Walsh DA. Mechanisms and targets of angiogenesis and nerve growth in osteoarthritis. Nat Rev Rheumatol 2012;8(7):390–8. https://doi.org/10.1038/nrrheum.2012.80.
[37] Tempfer H, Traweger A. Tendon vasculature in Health and disease. Front Physiol 2015;6:330. https://doi.org/10.3389/fphys.2015.00330.
[38] Tang C, Chen Y, Huang J, Zhao K, Chen X, Yin Z, et al. The roles of inflammatory mediators and immunocytes in tendinopathy. J Orthop Translat 2018;14:23–33. https://doi.org/10.1016/j.jot.2018.03.003.
[39] Annamalai RT, Turner PA, Carson WFt, Levi B, Kunkel S, Stegemann JP. Harnessing macrophage-mediated degradation of gelatin microspheres for spatiotemporal control of BMP2 release. Biomaterials 2018;161:216–27. https://doi.org/10.1016/j.biomaterials.2018.01.040.
[40] Łęgosz P, Drela K, Pulik Ł, Sarzyńska S, Małdyk P. Challenges of heterotopic ossification-Molecular background and current treatment strategies. Clin Exp Pharmacol Physiol 2018;45(12):1229–35. https://doi.org/10.1111/1440-1681.13025.
[41] Wang X, Li F, Xie L, Crane J, Zhen G, Mishina Y, et al. Inhibition of overactive TGF-β attenuates progression of heterotopic ossification in mice. Nat Commun 2018;9(1):551. https://doi.org/10.1038/s41467-018-02988-5.
[42] Yin Z, Chen X, Zhu T, Hu JJ, Song HX, Shen WL, et al. The effect of decellularized matrices on human tendon stem/progenitor cell differentiation and tendon repair. Acta Biomater 2013;9(12):9317–29. https://doi.org/10.1016/j.actbio.2013.07.022.
[43] Rui YF, Lui PP, Wong YM, Tan Q, Chan KM. Altered fate of tendon-derived stem cells isolated from a failed tendon-healing animal model of tendinopathy. Stem Cell Dev 2013;22(7):1076–85. https://doi.org/10.1089/scd.2012.0555.
[44] Li K, Deng Y, Deng G, Chen P, Wang Y, Wu H, et al. High cholesterol induces apoptosis and autophagy through the ROS-activated AKT/FOXO1 pathway in tendon-derived stem cells. Stem Cell Res Ther 2020;11(1):131. https://doi.org/10.1186/s13287-020-01643-5.
[45] Lin D, Alberton P, Caceres MD, Volkmer E, Schieker M, Docheva D. Tenomodulin is essential for prevention of adipocyte accumulation and fibrovascular scar

formation during early tendon healing. Cell Death Dis 2017;8(10):e3116. https://doi.org/10.1038/cddis.2017.510.
[46] Valer JA, Sánchez-de-Diego C, Gámez B, Mishina Y, Rosa JL, Ventura F. Inhibition of phosphatidylinositol 3-kinase α (PI3Kα) prevents heterotopic ossification. EMBO Mol Med 2019;11(9):e10567. https://doi.org/10.15252/emmm.201910567.
[47] Wang Y, He G, Wang F, Zhang C, Ge Z, Zheng X, et al. Aspirin inhibits adipogenesis of tendon stem cells and lipids accumulation in rat injury tendon through regulating PTEN/PI3K/AKT signalling. J Cell Mol Med 2019;23(11):7535–44. https://doi.org/10.1111/jcmm.14622.
[48] Agarwal S, Loder S, Brownley C, Cholok D, Mangiavini L, Li J, et al. Inhibition of Hif1α prevents both trauma-induced and genetic heterotopic ossification. Proc Natl Acad Sci U S A 2016;113(3):E338–47. https://doi.org/10.1073/pnas.1515397113.
[49] Hino K, Horigome K, Nishio M, Komura S, Nagata S, Zhao C, et al. Activin-A enhances mTOR signaling to promote aberrant chondrogenesis in fibrodysplasia ossificans progressiva. J Clin Invest 2017;127(9):3339–52. https://doi.org/10.1172/JCI93521.
[50] Bunpetch V, Zhang X, Li T, Lin J, Maswikiti EP, Wu Y, et al. Silicate-based bioceramic scaffolds for dual-lineage regeneration of osteochondral defect. Biomaterials 2019;192:323–33. https://doi.org/10.1016/j.biomaterials.2018.11.025.
[51] Kim D, Paggi JM, Park C, Bennett C, Salzberg SL. Graph-based genome alignment and genotyping with HISAT2 and HISAT-genotype. Nat Biotechnol 2019;37(8):907–15. https://doi.org/10.1038/s41587-019-0201-4.
[52] Li H. A statistical framework for SNP calling, mutation discovery, association mapping and population genetical parameter estimation from sequencing data. Bioinformatics 2011;27(21):2987–93. https://doi.org/10.1093/bioinformatics/btr509.
[53] Anders S, Pyl PT, Huber W. HTSeq–a Python framework to work with high-throughput sequencing data. Bioinformatics 2015;31(2):166–9. https://doi.org/10.1093/bioinformatics/btu638.
[54] Leng N, Li Y, McIntosh BE, Nguyen BK, Duffin B, Tian S, et al. EBSeq-HMM: a Bayesian approach for identifying gene-expression changes in ordered RNA-seq experiments. Bioinformatics 2015;31(16):2614–22. https://doi.org/10.1093/bioinformatics/btv193.
[55] Yu G, Wang LG, Han Y, He QY. clusterProfiler: an R package for comparing biological themes among gene clusters. OMICS 2012;16(5):284–7. https://doi.org/10.1089/omi.2011.0118.
[56] Subramanian A, Narayan R, Corsello SM, Peck DD, Natoli TE, Lu X, et al. A next generation connectivity Map: L1000 platform and the first 1,000,000 profiles. Cell 2017;171(6):1437–1452 e17. https://doi.org/10.1016/j.cell.2017.10.049.